Nuclear Technology

ISSN: (Print) (Online) Journal homepage: https://www.tandfonline.com/loi/unct20

Kilowatt Reactor Using Stirling TechnologY (KRUSTY) Component-Critical Experiments

Rene Sanchez , Travis Grove , David Hayes , Joetta Goda , George McKenzie , Jesson Hutchinson , Theresa Cutler , John Bounds , Jessie Walker , William Myers & Kristin Smith

To cite this article: Rene Sanchez , Travis Grove , David Hayes , Joetta Goda , George McKenzie , Jesson Hutchinson , Theresa Cutler , John Bounds , Jessie Walker , William Myers & Kristin Smith (2020) Kilowatt Reactor Using Stirling TechnologY (KRUSTY) Component-Critical Experiments, Nuclear Technology, 206:sup1, 56-67, DOI: 10.1080/00295450.2020.1722553

To link to this article: https://doi.org/10.1080/00295450.2020.1722553

Published online: 04 Jun 2020.

NUCLEAR TECHNOLOGY · VOLUME 206 · S56–S67 · 2020

DOI: https://doi.org/10.1080/00295450.2020.1722553

Kilowatt Reactor Using Stirling TechnologY (KRUSTY) Component-Critical Experiments

Rene Sanchez,* Travis Grove, David Hayes, Joetta Goda, George McKenzie, Jesson Hutchinson, Theresa Cutler, John Bounds, Jessie Walker, William Myers, and Kristin Smith

Los Alamos National Laboratory, Advanced Nuclear Technology, P.O. Box 1663, MS B228, Los Alamos, New Mexico 87545

Received October 2, 2019
Accepted for Publication January 24, 2020

Abstract — *A series of critical experiments were conducted at the National Criticality Experiments Research Center (NCERC) in Nevada to evaluate the operational performance of a compact reactor that eventually will resemble the flight unit the National Aeronautics and Space Administration will use for deep space exploration. The results from the experiments are compared to preliminary results from computational models using MCNP and ENDF/B-7.1 neutron cross-section data.*

Keywords — *Reactivity, k_{eff}, cents, β_{eff}, neutron cross section.*

Note — *Some figures may be in color only in the electronic version.*

I. INTRODUCTION

For more than 30 years, the National Aeronautics and Space Administration (NASA) has relied on radioisotope thermoelectric generators to produce the electricity that is used to power instrumentation in spacecraft or Rover vehicles deployed to other planets. In the 2000s, NASA decided to explore other sources of energy to produce electricity for spacecraft that will be used for a deep space exploration mission. In 2012, the National Criticality Experiments Research Center (NCERC) conducted a successful experiment that demonstrated how nuclear heating can be transferred with the use of a heat pipe into a Stirling engine and produce electricity.[1,2]

The main objective of the Kilowatt Reactor Using Stirling TechnologY[3–5] (KRUSTY) experiment was to evaluate the operational performance of a compact reactor that closely resembles the flight unit NASA will use for deep space exploration missions. In addition, the purpose of the experiments was to provide high-quality critical and reactor physics benchmarks that can be used to test neutron cross-section data used in steady-state and dynamic computer models. The component-critical experiment consisted of the core described below surrounded by a beryllium oxide (BeO) reflector and shield materials. As seen in Fig. 1, the radial BeO reflector and some of the shield materials [stainless steel and boron carbide (B_4C) plates] sit on the movable platen of the Comet vertical assembly machine. The stainless steel shield blocks sit on the top platform of Comet. There are axial BeO reflectors. One of them sits on the top of the core and the other one is below the core (see Fig. 1). There may be up to 2-in.-thick BeO plates in the shim pan located above the BeO radial reflector. Finally, the top chamber mount assembly and B_4C slabs sit on top of the stainless steel blocks. The assembly of the core and other hardware is described below.

To attain a supercritical state, the radial reflector and shield materials on the movable platen were raised to partially surround the core. To increase the reactivity in the experiment, more BeO plates were added to the radial

*E-mail: rgsanchez@lanl.gov

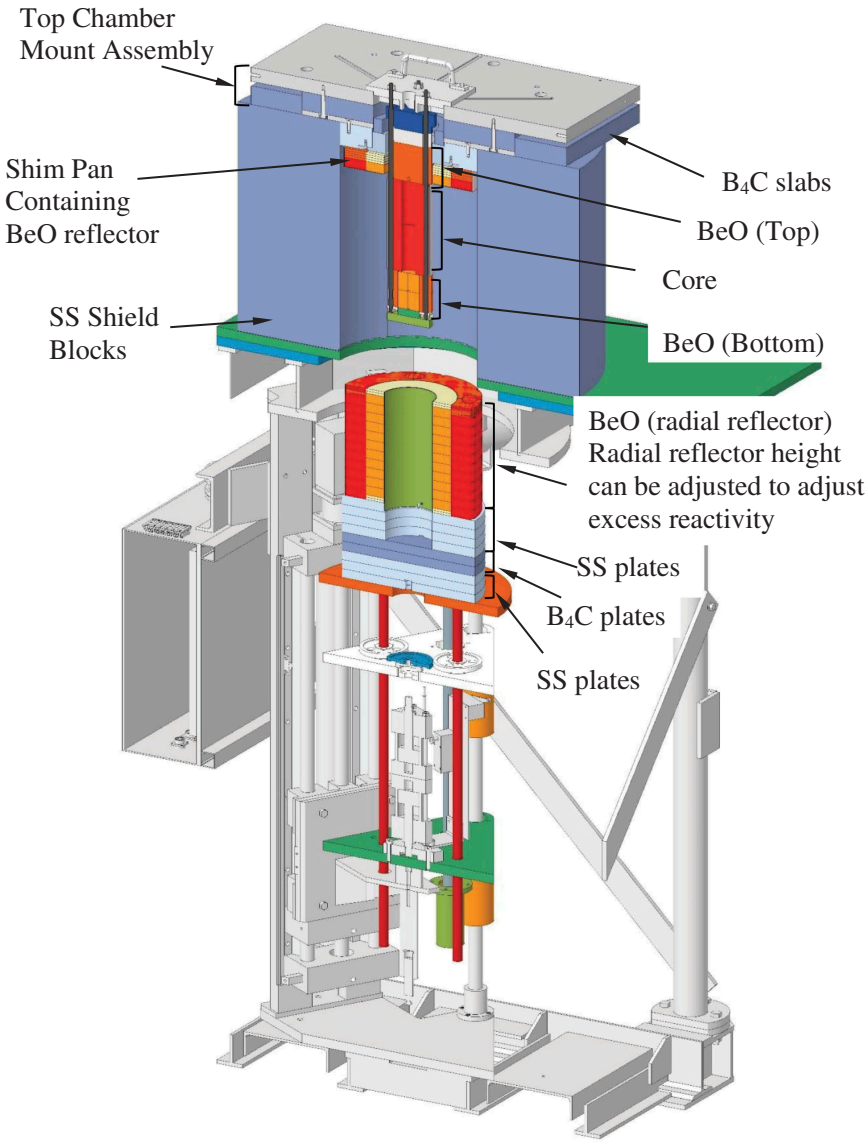

Fig. 1. Cross-section view of component-critical experiments (phase 1) (SS = stainless steel).

BeO on the movable platen, thus increasing the radial reflector height. The platen was raised and because more neutrons were reflected back into the core, the reactivity of the experiment increased.

The KRUSTY project was divided into four phases. The objective of phase 1 (component critical) and phase 2 (cold critical) was to assess the bias of the k_{eff} due to the BeO neutron cross-section data and to determine the reactivity worth of the B_4C control rod that may be used in the flight unit that NASA may deploy to other planets. Phase 3 was the warm-critical runs that provided key parameters used in the modeling of the neutronic and thermal-dynamic behavior of the KRUSTY experiment. The data obtained in the previous phases were used in the high-temperature 28-h run (phase 4). As stated above, the experiments in phase 1 consisted of the fuel reflected with BeO and the stainless steel shield. The experiments in phases 2, 3, and 4 consisted of the fuel embedded in a vacuum chamber with eight heat pipes attached to the periphery of the fuel. Similar to phase 1, the fuel in the vacuum chamber was reflected by BeO and the stainless steel shield. This paper describes the experiment and the results obtained during the execution of phase 1 (component-critical) experiments. A comparison between experimental and preliminary computational results is presented.

II. DESCRIPTION OF THE COMPONENT-CRITICAL EXPERIMENT

The component-critical experiment was composed of a 32-kg uranium alloy (~7.65 wt% Mo) core with a calculated density of ~17.35 ± 0.02 g/cm^3 at room temperature. The uranium was isotopically enriched to 93 wt%. The uranium core components (three of them) form the shape of an upright cylindrical annulus with an inner diameter of 4 cm and an outer diameter of 11 cm. Table I shows the weights and isotopic composition of each of the three core components. The uranium core had a height of 25 cm. The three core pieces had eight grooves equally spaced on the radial surfaces that extended axially to accommodate heat pipes. The core was cast and machined at the U.S. Department of Energy's (DOE's) Y-12 National Security Complex. The heat pipes were not used as part of the component-critical experiments. The inner hole in the uranium core was designed to accommodate a B_4C control rod. Segments of the B_4C control rod were inserted in the uranium core during the phase 1 critical experiments to obtain the reactivity worth of the control rod.

Figures 2 through 5 show the KRUSTY component-critical hardware used during the execution of (phase 1) component-critical experiments. As seen in Figs. 2 through 5, the bottom axial BeO reflector containing the two BeO plugs was slid through the stainless steel rods and placed on top of the retaining plate, followed by the fuel. An AmBe neutron source was placed in the center of the fuel to induce fission neutrons and to better measure the true multiplication of the configurations. The neutron source was not always present for some of the configurations. The top axial BeO reflector was slid through the rod and placed on top of the fuel followed by one stainless steel and one B_4C shield piece. The bottom and top axial BeO reflectors and the shield pieces had eight grooves equally spaced on their radial surfaces to accommodate heat pipes, similar to the fuel components. An aluminum sleeve or jacket was placed over the fuel. The rods seen in Fig. 2 with reflectors, fuel, and shield pieces were attached to a squared hanger plate. The assembled core with axial reflectors and shield pieces was lowered through the chamber mount assembly plate and firmly secured (see Fig. 5). Stainless steel shield blocks were also mounted on the top platform of the Comet assembly (see Fig. 6). It should be noted that the reactivity of the experiment was controlled by raising or withdrawing the BeO radial reflector, which was mounted on the movable platen (see Fig. 7).

TABLE I

Weights and Isotopic Composition of the Three Components that Form the Core

	Top	Middle	Bottom
Weight (g)	10 741	10 718	10 741
^{234}U (wt%)	1.010	1.031	1.0147
^{235}U (wt%)	93.099	93.0297	93.0947
^{236}U (wt%)	0.4073	0.559	0.425
^{238}U (wt%)	5.483	5.38	5.4663
Mo (ppm)	75 600	77 867	76 000

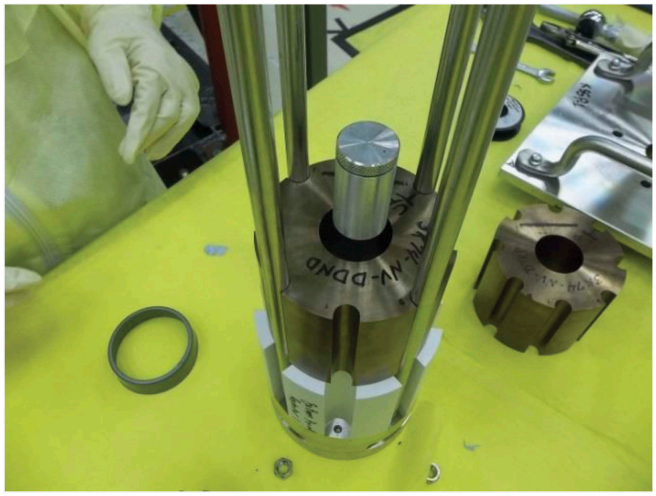

Fig. 2. Bottom BeO reflector and one uranium core component. Neutron source is in the aluminum capsule.

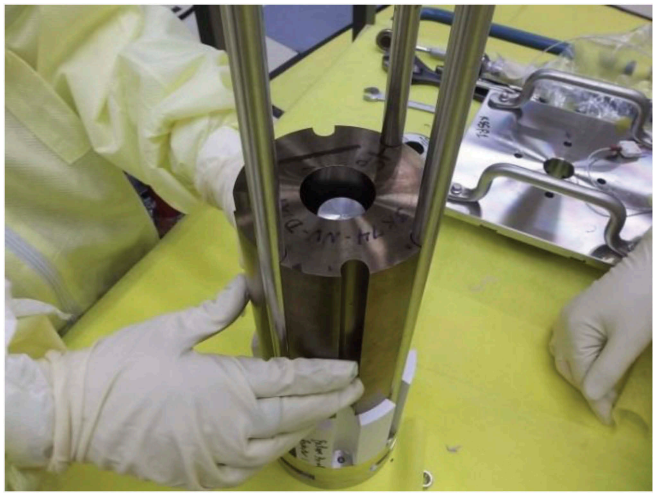

Fig. 3. BeO bottom reflector and two uranium core components.

The 304 stainless steel bore shield top that sat on top of the top BeO axial reflector had an outer diameter of 12.7 cm and a height of 3.8 cm. The purpose of this piece was to shield instrumentation and hardware on top of the core against gamma radiation.

Fig. 4. Bottom axial reflector of BeO and three core uranium components.

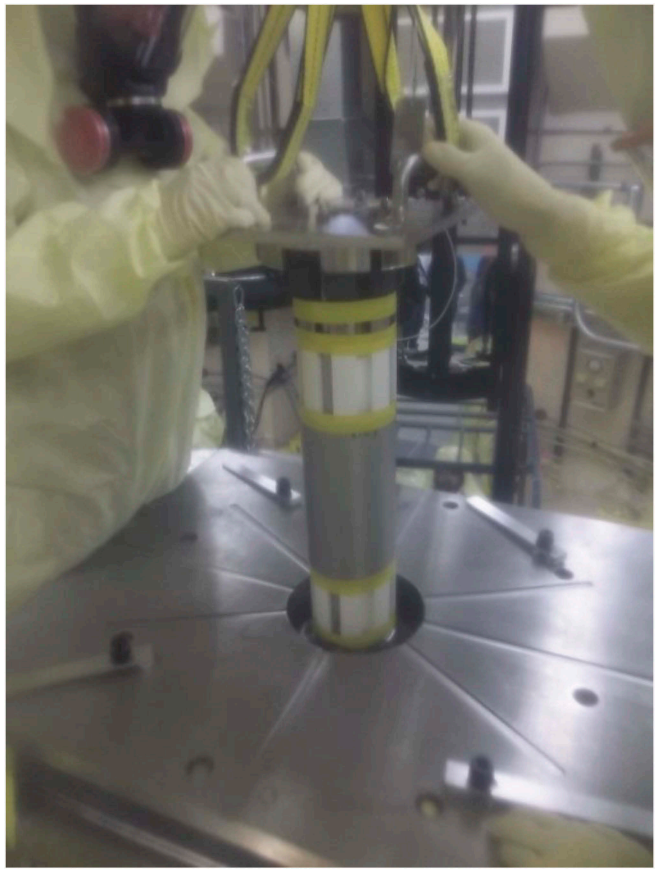

Fig. 5. Core and reflector components being lowered through the chamber mount assembly.

The B_4C bore shield top sat on top of the 304 stainless steel bore shield top. Its purpose was to shield instrumentation and hardware on the top of the core against neutron radiation. This piece had an outer diameter of 14.6 cm, a step diameter of 12.7 cm, and was 1.9 cm deep. The overall height was 5.1 cm.

The square hanger plate was made of 304 stainless steel. It was a 1.3-cm-thick, 25.4-cm-square plate with a 20.9-cm-diameter central protrusion that was 3.5 cm thick.

The BeO reflector was divided into three parts: the upper and lower axial reflectors and the radial reflector. The upper and lower axial BeO reflectors were part of the assembled core components described above. Each of the upper and lower axial BeO reflectors was 12.7 cm in diameter and 10.2 cm in height and had grooves to accommodate heat pipes. The radial reflector was made up of rings of different thicknesses to be able to limit the excess reactivity of the experiment. The inner side reflector rings had an inner diameter of approximately 14.5 cm and an outer diameter of 25.4 cm. The outer rings were divided into four parts. When assembled, the outer side reflector rings had an inner diameter of 25.4 cm and an outer diameter of 38.1 cm. Hazards associated with handling the BeO reflector parts were analyzed and appropriate controls were in place to minimize personnel exposure. The average calculated density of the BeO parts was 2.82 ± 0.016 g/cm^3.

The 304 stainless steel shield (shown in Figs. 6 and 7) was also divided into three parts: the radial shield, the lower shield, and the top chamber mount assembly.

The radial shield was divided into four parts. When assembled, the radial shield had an inner diameter of 40.6 cm and an outer diameter of 101.6 cm. The radial shield was approximately 66 cm in height.

The lower 304 stainless steel shield sat on the movable platen and had a layer of B_4C to absorb neutrons that leak from the core. The bottom 304 stainless steel shield and the B_4C had a diameter of 39.7 cm. The bottom part of the 304 stainless steel shield that sat on the movable platen had three plates with a total height of approximately 7.5 cm. The B_4C layer sat on the top of the bottom 304 stainless steel shield and was composed of two plates with a total height of 5.1 cm. Another four 304 stainless

steel shield plates sat on top of the B_4C layer with an approximate inner diameter of 14 cm, an outer diameter of 39.7 cm, and a total height of 10.2 cm. The top chamber mount assembly was composed of a 304 stainless steel leveling plate, a B_4C leveling plate, a 304 stainless steel lower leveling plate, B_4C side bars, a 304 stainless steel outer top ring shield, and a 304 stainless steel inner top ring shield (shown in Fig. 8). The 304 stainless steel upper leveling plate was 76.2 cm wide × 4.0 cm long × 3.81 cm thick with a 21.0-cm-diameter central hole. The B_4C leveling plate was 63.5 cm wide × 76.2 cm long × 5.1 cm thick with a 21.0-cm-diameter central hole. The 304 stainless steel lower leveling plate was 63.5 cm wide × 76.2 cm long × 1.3 cm thick with a 21.0-cm central hole.

Fig. 6. Stainless steel shields and chamber mount assembly plate on top of the Comet assembly.

Fig. 7. BeO (white) radial reflector mounted on the movable platen of the Comet vertical assembly machine. Also, bottom 304 stainless steel shield (silver) with a layer of B_4C (dark).

There were two B_4C side bars. Each B_4C side bar was 76.2 cm long × 15.2 cm wide × 5.1 cm thick. The 304 stainless steel outer top ring shield had an outer diameter of 41.0 cm, an inner diameter of approximately 21.6 cm, and a thickness of 6.4 cm. Finally, the 304 stainless steel inner top ring shield had an inner diameter of 14.0 cm, an outer diameter of 21.6 cm, and a thickness of 4.5 cm. As seen in Fig. 8, this piece had a flange at one end that extended to a 30.5-cm outer diameter and was 1.0 cm thick with an inner diameter of 14.0 cm. The average calculated density of the 304 stainless steel parts was 7.95 ± 0.2 g/cm^3.

All B_4C parts except the discs used as part of the control rod were made using natural boron. The average calculated density of the B_4C parts with natural boron was 1.86 ± 0.01 g/cm^3. The segments used as part of the control rod were made of enriched boron containing up to 90 wt% ^{10}B. The B_4C discs used as part of the control rod had an inner diameter of 0.635 cm and an outer diameter of 3.81 cm. Some of the discs were 1.27 cm thick while others were approximately 0.32 cm thick (see Fig. 9). The average density for the enriched B_4C discs was 2.12 ± 0.05 g/cm^3.

A detailed description of the parts mentioned above with their manufacturing tolerances, weights, material uncertainties, etc., is given in a document entitled "KRUSTY:

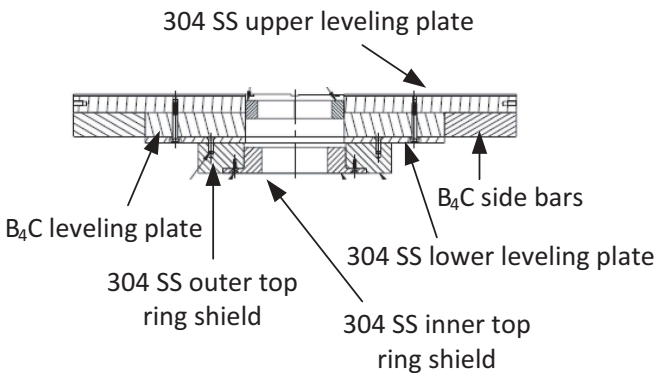

Fig. 8. Top chamber mount assembly (SS = stainless steel).

Fig. 9. B_4C (black discs) control rod being inserted into the center of the core. Also shown in the picture are the BeO plugs (white cylinders).

Beryllium-Oxide and Stainless-Steel Reflected Cylinder of HEU Metal," HEU-MET-FAST-101, which was submitted to the International Criticality Safety Benchmark Evaluation Project (ICSBEP) in October 2019 for review.[6]

A resistance temperature detector was installed midpoint on the outer surface of the fuel to measure the temperature of the core and to ensure that the measured temperature is within the limits specified in the experiment plan.

The component-critical experiments were performed on the Comet vertical assembly machine. This machine consists of a drive assembly and a stationary support structure (see Fig. 1). The BeO radial reflectors were mounted on the drive assembly and raised by a hydraulic lift and a ball screw linear motion driven by a stepper motor. Four ^3He neutron startup detectors were positioned approximately 3 to 4 m from the assembly to monitor the neutron leakage from the assembly. A 1/M as a function of radial reflector height was performed to estimate the reflector height at which the configuration will go critical.

III. RESULTS

Table II shows the configurations that were performed as part of the component-critical experiments (phase 1). A brief description of each configuration is given in the first column of Table II, followed by the BeO radial reflector height, the height of BeO in the shim pan (see Fig. 1), the B_4C control rod height, the measured k_{eff}, the calculated k_{eff}, the difference between calculated and measured (experiment) k_{eff}s, and the temperature of the configuration. There were 60 configurations that were performed during the phase 1 component-critical experiments. The average temperature for all the configurations was 16.3ºC. These experiments were performed between November 2017 and January 2018.

The neutron transport computer code MCNP6.2® (Ref. 7)[a] was used to calculate the k_{eff} for each configuration. A total of 25 million neutron histories were run for each configuration. The MCNP simulations used ENDF/B-VII neutron cross-section data. Neutron cross sections and the S(α, β) thermal scattering kernel for BeO were at 26.85ºC (300 K). The baseline MCNP model[8] is shown in Fig. 10. This detailed model was created using measured data that were provided by the manufacturer for each piece including the impurities.[6] The MCNP model assumed that the core was perfectly centered with respect to the radial BeO reflector and there were no axial gaps in the radial reflector. The uncertainty in k_{eff} associated with the alignment of the central core column, alignment of the platen, and axial gaps between the radial BeO reflector rings is given in Ref. 6. It is important to note that the calculated k_{eff}'s shown in Table II are preliminary and they may change as the detailed model continues to evolve.

For all the configurations in Table II that showed a measured k_{eff} greater than 1, an exponential rise in the neutron population was observed. The data are fitted and a reactor period is determined. The reactor period is then input into the Inhour equation,[9] and from this equation the reactivity of the configuration is found. To convert reactivity into k_{eff}, a β_{eff} of 0.00711 ± 0.0002 was used. The β_{eff} was calculated using the KOPTS (Ref. 6) card in MCNP.

Configurations 1 and 10 are considered baseline cases and in both cases MCNP calculates about 365 pcm below the measured k_{eff}. Configuration 2 compares how reproducible the measured k_{eff} is of the configuration assembled in configuration 1 by unstacking part of the radial reflector and then putting it back again. As seen in Table II, there is a small difference in the measured k_{eff} between configurations 1 and 2 mainly due to the alignment of the last 1/4-in.-thick BeO radial reflector plate. This alignment issue was partially corrected in configuration 7 and completely corrected in configuration 10. The difference in the measured k_{eff}'s between configurations 1, 7, and 10 is quite small.

[a] MCNP® and Monte Carlo N-Particle® are registered trademarks owned by Triad National Security, LLC, manager and operator of Los Alamos National Laboratory. Any third party use of such registered marks should be properly attributed to Triad National Security, LLC, including the use of the designation as appropriate. For the purposes of visual clarity, the registered trademark symbol is assumed for all references to MCNP within the remainder of this paper.

TABLE II

Measured and Calculated k_{eff} for KRUSTY Component-Critical Experiments

Sequential Operations Configuration	BeO Height (in.)	Shim BeO (in.)	B_4C Height (in.)	k_{eff} Measured	k_{eff} Calculated	(C-E)[a]	Core Temperature (°C)
1. Baseline initial critical	11.25	0	0	1.00067545	0.99702 ± 0.00015	−0.00366	15.0
2. Unload and reload 4 in. of BeO	11.25	0	0	1.00049059	0.99702 ± 0.00015	−0.00347	15.7
3. No change	11.25	0	0	1.00049059	0.99702 ± 0.00015	−0.00347	15.6
4. Only top source plug removed	11.25	0	0	1.00048348	0.99722 ± 0.00015	−0.00326	15.6
5. Only bottom source plug removed	11.25	0	0	1.0004977	0.99711 ± 0.00015	−0.00339	15.6
6. Both source plugs removed	11.25	0	0	1.00049059	0.99716 ± 0.00015	−0.00333	15.6
7. Source plugs replaced (baseline)	11.25	0	0	1.00060435	0.99702 ± 0.00015	−0.00358	14.8
8. Added 1/8 in. BeO	11.375	0	0	1.00366876	1.00013 ± 0.00015	−0.00354	14.8
9. No change	11.375	0	0	1.003555	1.00013 ± 0.00015	−0.00343	15.0
10. Removed 1/8 in. BeO (baseline)	11.25	0	0	1.00065412	0.99702 ± 0.00015	−0.00363	15.4
11. Removed source and source holder	11.25	0	0	1.00016353	0.99658 ± 0.00015	−0.00358	15.7
12. No change	11.25	0	0	1.00016353	0.99658 ± 0.00015	−0.00358	15.2
13. Added 1/8 in. BeO	11.375	0	0	1.00321372	0.99953 ± 0.00015	−0.00368	15.3
14. Added Al source holder (no neutron source)	11.375	0	0	1.00332748	0.99977 ± 0.00015	−0.00356	15.8
15. No change	11.375	0	0	1.00342702	0.99977 ± 0.00015	−0.00366	15.3
16. Removed 1/8 in. BeO	11.25	0	0	1.0003555	0.99698 ± 0.00015	−0.00338	15.3
17. No change	11.25	0	0	1.00036972	0.99698 ± 0.00015	−0.00339	15.5
18. Removed source holder can, source holder rod present (no source)	11.25	0	0	1.00029151	0.99694 ± 0.00015	−0.00335	15.9
19. Removed source holder rod and placed source in the top source plug location	11.25	0	0	1.00031284	0.99679 ± 0.00015	−0.00352	15.9
20. No change	11.25	0	0	1.00034128	0.99679 ± 0.00015	−0.00355	15.7
21. Source moved to bottom source plug location	11.25	0	0	1.00033417	0.99696 ± 0.00015	−0.00337	15.7
22. Open and close shield door	11.25	0	0	1.00038394	0.99696 ± 0.00015	−0.00342	15.7
23. Removed source, installed bottom source plug, and added 1/8 in. BeO	11.375	0	0	1.00343413	0.99953 ± 0.00015	−0.0039	15.8
24. No change	11.375	0	0	1.00344124	0.99953 ± 0.00015	−0.00391	15.7
25. Replaced upper bottom axial BeO reflector plug with Al plug	11.375	0	0	1.00047637	0.99661 ± 0.00015	−0.00387	15.8

(Continued)

TABLE II (Continued)

Sequential Operations Configuration	BeO Height (in.)	Shim BeO (in.)	B_4C Height (in.)	k_{eff} Measured	k_{eff} Calculated	(C-E)[a]	Core Temperature (°C)
26. Replaced lower bottom axial BeO reflector plug with Al plug	11.375	0	0	1.00228942	0.99868 ±0.00015	−0.00361	16.0
27. No change	11.375	0	0	1.00238185	0.99868± 0.00015	−0.0037	15.9
28. Replaced both (lower and upper) axial BeO plugs	11.375	0	0	<1	0.99536 ± 0.00015	–	16.1
29. Added 1/8 in. BeO and replaced both bottom BeO axial reflector plugs with Al plugs	11.5	0	0	1.00199791	0.99833 ± 0.00015	−0.00367	16.1
30. Added new diagnostic bottom with stainless steel threaded rod, replaced Al plugs with BeO, and removed 1/8 in. BeO	11.375	0	0	1.00337014	0.99950 ± 0.00015	−0.00387	16.4
31. Steel bolts in diagnostic bottom	11.375	0	0	1.00340569	0.99950 ± 0.00015	−0.00391	15.6
32. Removed 1/8 in. BeO	11.25	0	0	1.0003555	0.99669 ± 0.00015	−0.00367	15.6
33. Added 1/8 in. BeO	11.375	0	0	1.0034128	0.99950 ± 0.00015	−0.00391	15.7
34. No change	11.375	0	0	1.0034128	0.99950 ± 0.00015	−0.00391	15.7
35. Added 1/8 in. B_4C to control rod	11.375	0	0.125	1.00120159	0.99751 ± 0.00015	−0.00369	15.9
36. Added 1/8 in. B_4C to control rod for a total of 1/4 in. B_4C and added 1/8 in. BeO. Neutron source is on top source plug location.	11.5	0	0.25	1.00321372	0.99940 ± 0.00015	−0.00381	16.0
37. Added 1/8 in. B_4C to control rod	11.5	0	0.375	1.00236763	0.99862 ± 0.00015	−0.00375	16.1
38. Added 1/8 in. B_4C to control rod	11.5	0	0.5	1.00152865	0.99765 ± 0.00014	−0.00388	16.2
39. No change	11.5	0	0.5	1.00152865	0.99765 ± 0.00014	−0.00388	15.8
40. Removed four (1/8 in. B_4C) and replaced by one (1/2 in. B_4C)	11.5	0	0.5	1.0015642	0.99795 ± 0.00015	−0.00361	15.9
41. Added 1/8 in. B_4C to control rod	11.5	0	0.625	1.00088875	0.99742 ± 0.00015	−0.00347	16.0
42. Added 1/8 in. BeO	11.625	0	0.625	1.0038394	1.00001 ± 0.00015	−0.00383	16.0
43. Added 1/8 in. B_4C to control rod	11.625	0	0.75	1.00309285	0.99934 ± 0.00015	−0.00375	16.2
44. Reshuffled core pieces and removed 3/8 in. BeO and 0.75 in. B_4C from control rod	11.25	0	0	1.000711	0.99710 ± 0.00015	−0.00361	16.1
45. Added empty shim pan	11.25	0	0	1.0012798	0.99753 ± 0.00015	−0.00375	15.7
46. Added 2 in. of BeO to shim pan	10.375	2	0	1.00330615	1.00100 ± 0.00015	−0.00231	15.8
47. Removed 1/8 in. BeO from radial reflector	10.25	2	0	1.00000711	0.99737 ± 0.00015	−0.00264	15.8

(Continued)

TABLE II (Continued)

Sequential Operations Configuration	BeO Height (in.)	Shim BeO (in.)	B_4C Height (in.)	k_{eff} Measured	k_{eff} Calculated	(C-E)[a]	Core Temperature (°C)
48. Added ^{3}He detectors around the core and added 1/8 in. BeO	10.375	2	0	1.002844	1.00120 ± 0.00015	−0.00164	17.4
49. Removed ^{3}He detector, added 1 in. B_4C to control rod, and added 1/4 in. BeO	10.625	2	1	1.00295776	1.00163 ± 0.00015	−0.00133	17.7
50. No change	10.625	2	1	1.00297198	1.00163 ± 0.00015	−0.00134	17.5
51. Added 1/8 in. B_4C to control rod	10.625	2	1.125	1.00222543	1.00090 ± 0.00015	−0.00133	17.8
52. Added 7/8 in. B_4C to control rod and 1/8 in. BeO to radial reflector	10.75	2	2.0	1.00024885	0.99894 ± 0.00014	−0.00131	17.7
53. Added 1/8 in. BeO to radial reflector	10.875	2	2.0	1.00401004	1.00253 ± 0.00015	−0.00148	17.7
54. Added 1/8 in. B_4C to control rod	10.875	2	2.125	1.00312129	1.00171 ± 0.00015	−0.00141	17.8
55. No change	10.875	2	2.125	1.00306441	1.00171 ± 0.00015	−0.00135	19.6
56. Added 1/4 in. B_4C to control rod	10.875	2	2.375	1.0009954	0.99971 ± 0.00015	−0.00129	19.8
57. Added 1/8 in. B_4C to control rod	10.875	2	2.5	1.00002133	0.99899 ± 0.00015	−0.00103	19.9
58. Added 1/8 in. BeO to radial reflector	11.0	2	2.5	1.0037683	1.00241 ± 0.00015	−0.00136	19.1
59. Added 1/8 in. BeO to radial reflector and 1/2 in. B_4C to control rod	11.125	2	3.0	1.0031284	1.00248 ± 0.00015	−0.00065	19.0
60. Added 1/4 in. BeO to radial reflector and 1 in. B_4C to control rod	11.375	2	4.0	1.0007821	1.00061 ± 0.00015	−0.00017	19.0

[a](C-E) = Calculated k_{eff} –Experimental k_{eff}.

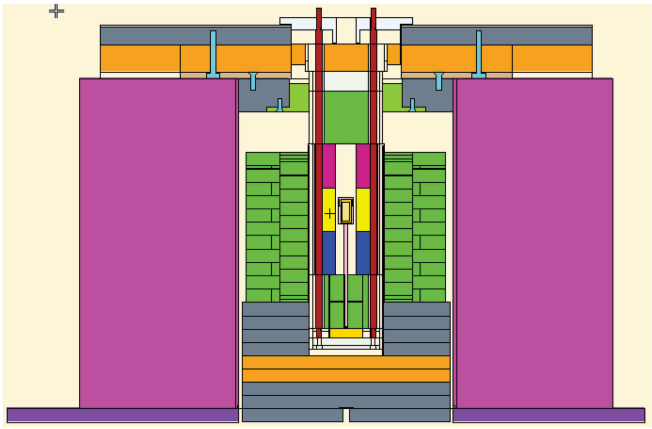

Fig. 10. MCNP model of KRUSTY.

Configurations 4, 5, and 6 investigated the effects in the reactivity, and for that matter in the k_{eff} of removing the top, the bottom, or both stainless steel shield plugs shown in Fig. 11. Measured and calculated k_{eff} values showed no significant effect.

Configuration 11 investigated the reactivity effect of removing the AmBe neutron source and the aluminum source holder. As seen in Table II, removing the AmBe neutron source and the source holder removed about 51 pcm when compared to configuration 1. The MCNP simulations also confirmed the loss of reactivity due to the removal of source and source holder.

Configurations 8, 10, 13, 16, 23, 29, 32, and 33 determined the reactivity worth per mil of adding the BeO radial reflector to the assembly. The reactivity per mil varied from 2.32 to 2.64 pcm/mil. This measurement was very important because it allows us to estimate the BeO reflector thickness that was needed to have enough excess reactivity to heat the fuel up to 800°C for the high-temperature 28-h run (phase 4).

Configurations 3, 9, 12, 15, 17, 20, 24, 27, 34, 39, 50, and 55 are the "no change" configurations, meaning that they are the same as the previous configurations. For example, configuration 15 was the same as configuration 14; configuration 3 was the same as configuration 2, and so on. The main objective of these measurements was to demonstrate the reproducibility of the reactivity measurements.

Configurations 14, 18, 19, and 21 investigated the reactivity addition or subtraction due to adding or retrieving the aluminum source holder and source holder rods to/from the center of the core or placing the neutron source in the top or bottom source plug location (see Fig. 11). As seen in Table II, the changes described above added or subtracted between 1 and 14 pcm of reactivity.

Configuration 22 investigated the reproducibility in reactivity of opening and closing the stainless steel shield door. As illustrated in Table II, this action represents a difference of 5 pcm between the reactivity in this configuration and that of configuration 21.

Configurations 25, 26, and 28 investigated the reactivity effects of replacing the top and/or bottom BeO reflector plugs with aluminum plugs. Measured and calculated k_{eff}'s showed the same trend, although for configurations 25 and 26 the calculated k_{eff}'s are about 375 pcm on average below the measured k_{eff}'s. Note that in configuration 28, replacing both BeO plugs with aluminum plugs (see Table II), was subcritical.

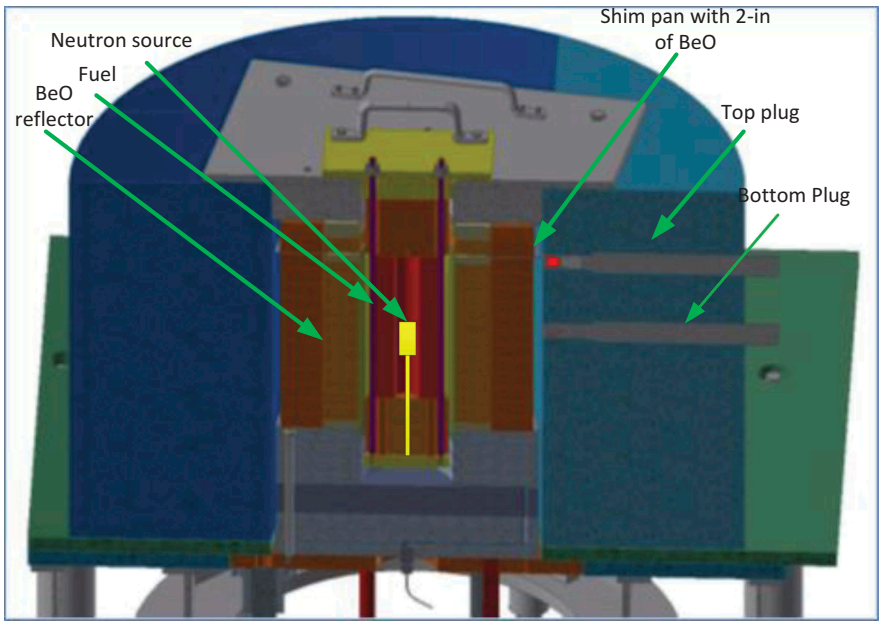

Fig. 11. Component-critical experiment (phase 1).

In configurations 30 and 31 a new diagnostic bottom replaced the old diagnostic bottom. A stainless steel threaded rod was added to the new diagnostic bottom. This change made a very small difference in reactivity (configurations 30 and 31 compared to 14).

Configuration 44 explored the reactivity effects of reshuffling the three core pieces. As seen in Table II, a small reactivity difference was found between this configuration and configuration 1 (baseline).

Configuration 45 investigated the reactivity effect of adding an empty shim pan to the experiment (see Fig. 10). Adding the empty shim pan had a positive reactivity effect (~60 pcm) compared to the baseline case (configuration 1). The simulations predicted an increase of reactivity of 51 pcm.

Configuration 46 investigated the reactivity effect of adding a 2-in.-thick BeO reflector to the shim pan. As seen in Fig. 10, the shim pan was located near the top part of the core. The addition of BeO to the shim pan added a considerable amount of reactivity, such that the radial reflector height had to be reduced from 11.25 to 10.375 in. (see Table II) in order to be within the 80-¢ (569 pcm) technical safety requirement limit. According to Table II, the measured reactivity was approximately 331 pcm compared to 100 pcm from simulations.

In configuration 47, a 1/8-in.-thick BeO radial reflector was removed from configuration 46 and the reactivity was measured to be 0.1 ¢ (0.711 pcm). The simulation predicted 264 pcm below the measured reactivity.

Configuration 48 investigated the reactivity effect of adding four small ^{3}He detectors to the periphery of the core. The addition of the ^{3}He detectors reduced reactivity by approximately 6 ¢ (43 pcm) compared to configuration 46.

Configurations 35 through 43 and 49 through 60 investigated the reactivity effects of adding segments of B_4C in the center of the core with no BeO in the shim pan and with 2-in.-thick BeO in the shim pan (see Fig. 8). Based on these measurements, the integral worth curve as a function of control rod height is shown in Fig. 12. It is important to note that the central control rod proposed by NASA will have enough negative reactivity worth to shut down a reactor that would have 3.00 $ (2133 pcm) of excess reactivity.

Finally, it should be noted that as the temperature of the room where the experiments were conducted increased, the difference between the calculated and measured k_{eff}'s got smaller (see Table II). A possible explanation is that the neutron cross sections and the thermal S(α, β) used in the MCNP models were evaluated at 300 K, while the majority of the experiments were executed in a room at a temperature of 15°C (288 K).

IV. CONCLUSIONS

A total of 60 configurations were performed as part of component-critical (phase 1) experiments. For the baseline configuration, the calculated k_{eff} was 366 pcm below the measured k_{eff}. An integral worth curve as a function of control rod height was attained. These data will be extremely useful because the proposed control rod that NASA will use in the

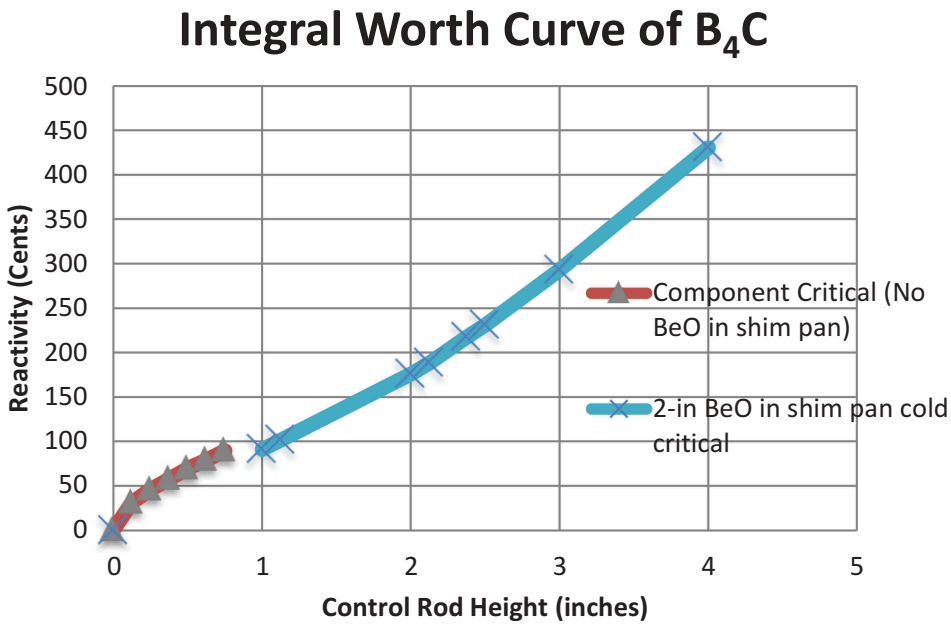

Fig. 12. Integral worth curve of B_4C control rod.

flight unit is very similar to the one used in these experiments. Finally, it appears that as the temperature of the room where the critical experiments were being conducted increased, the difference in calculated and experimental k_{eff}'s decreased substantially.

V. FUTURE WORK

The intent of this paper was to document the experiments that were conducted as part of phase 1 and to compare them with preliminary simulations. A report entitled "KRUSTY: Beryllium-Oxide and Stainless-Steel Reflected Cylinder of HEU Metal," HEU-MET-FAST-101, which has been summited to the ICSBEP for review, documents in great detail all the components used in these experiments. This report also discusses the uncertainties in k_{eff} associated with the uncertainties of the masses and manufacturing and machining tolerances of all the parts used in the experiments. A paper summarizing these results will be submitted to the *Nuclear Technology* journal in the near future.

Acknowledgments

This work is supported by the NASA Space Technology Program and in part by the DOE Nuclear Criticality Safety Program, funded and managed by the National Nuclear Security Administration for the DOE.

References

1. R. G. SANCHEZ, et al., "MCNP Simulations in Support of the Heat Pipe in Flattop Experiment," LA-UR-13-20495, Los Alamos National Laboratory (Oct. 2013).
2. D. I. POSTON, "Criticality and Dynamic Benchmarking of the DUFF Reactor Test," LA-UR-13-20724, Los Alamos National Laboratory (Oct. 2013).
3. D. I. POSTON, "KRUSTY Design and Modelling," LA-UR -16-28377, Los Alamos National Laboratory (Nov. 2016).
4. D. I. POSTON, "KRUSTY Test Results," LA-UR-18-23685, Los Alamos National Laboratory (Apr. 2018).
5. D. I. POSTON et al., "Design of the KRUSTY Reactor," *Proc. Topl. Mtg. Nuclear and Emerging Technologies for Space*, pp. 58–61, American Nuclear Society (2018).
6. K. N. SMITH, et al., "KRUSTY: Beryllium-Oxide and Stainless-Steel Reflected Cylinder of HEU Metal," HEU-MET-FAST-101, Nuclear Energy Agency/OECD (Organization for Economic Co-operation and Development) (October 2019).
7. D. B. PELOWITZ, et al., "MCNP6 User's Manual," LA-CP -14-00745, Los Alamos National Laboratory (June 2014).
8. K. N. SMITH et al., "Preliminary Benchmark Analysis of Component Critical Configuration of KRUSTY," *Trans. Am. Nucl. Soc.*, **119**, 819 (2018).
9. G. R. KEEPIN, *Physics of Nuclear Kinetics*, Addison-Wesley Publishing Company, Inc., Reading, Massachusetts (1965).